

Laboratoire des Structures Métalliques Résilientes RESSLab

Téléphone : +41 21 693 24 27
Fax : +41 21 693 28 68
E-mail : dimitrios.lignos@epfl.ch
Site web : http://resslab.epfl.ch
Address: EPFL ENAC IIC RESSLAB
GC B3 485, Station 18,
CH-1015 Lausanne

Project #3: Multi-degree-of-freedom (MDoF) systems – SOLUTION

PART 1 – Modal analysis

<u>Numerical modelling approximations</u>: The 2-story MOLA building model consists of two moment resisting frames (MRFs) acting in parallel. The corresponding idealization of the multi-degree-of-freedom (MDOF) system as a 2D structure comprised of beam column elements is shown in Figure 1. Specifically, Figure 1a shows the node and element numbering for a single MRF. In the general case, each of the six nodes has three DOFs – two translations in the plane of the frame as well as one rotation. This yields a total of eighteen DOFs for the system.

Since the nodes 1 and 2 are fully fixed, their displacements are known (they equal zero) which leaves twelve unknown DOFs. A further simplification is possible by recognizing that the slabs located at each of the stories are rigid in the plane. As such, they provide a kinematic constraint for the nodes of the same stories. In other words, they link the node 3 with node 4 and node 5 with node 6 so that their lateral (horizontal) displacements are equal. This leaves ten unknown DOFs.

Finally, if we assume that the axial stiffness of the short springs that are acting as columns is much higher compared to their bending stiffness, we can remove the vertical DOFs from the list of the unknowns. This is because assuming columns to have an infinite axial stiffness effectively means that all vertical displacements are zero. This can be a good approximation in this case, particularly since the earthquake ground motion is only acting in the horizontal direction. As such, there are six DOFs used for static analysis (Figure 1b).

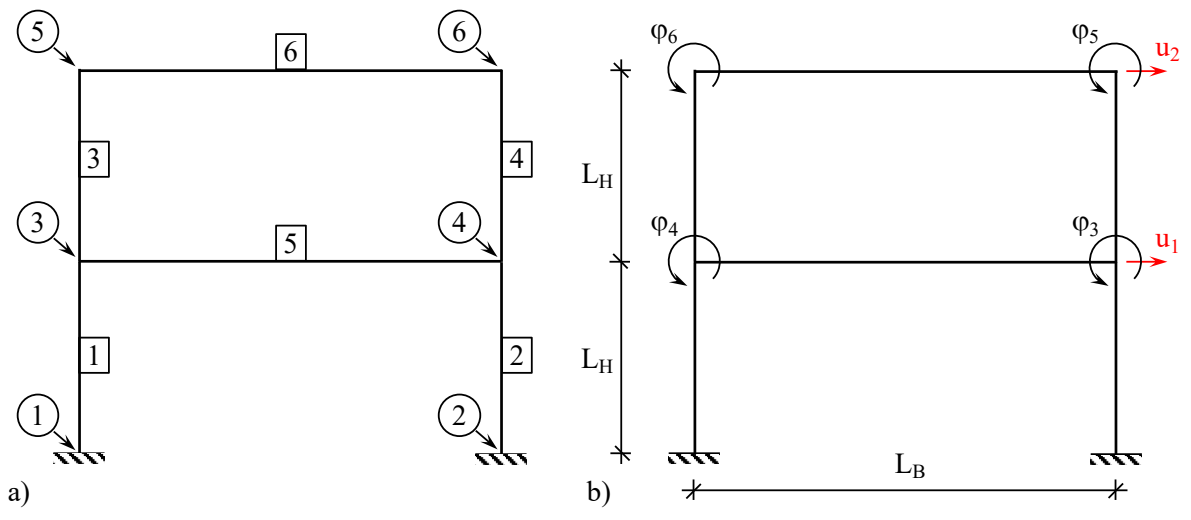


Figure 1. 2-story MRF structure: a) sketch of the model with node and element numbers written inside circles and rectangles, respectively; b) degrees of freedom (DOFs) of the MDOF

system - there are six DOFs for static analysis and the two DOFs used in dynamic analysis are highlighted in red.

To identify the dynamic DOFs, note that most of the mass is located at each of the floors. As a result, the mass can be lumped, i.e., assumed to exist only at each of the floors. Given that the earthquake ground motion acts at the supports in the horizontal direction, there are two DOFs used for the dynamic analysis. Specifically, the dynamic DOFs are lateral displacements of the first and second floor as indicated with u_1 and u_2 in red text in Figure 1b, respectively. In summary, for structural analysis the matrices will be 6x6 while for the dynamic response computations the matrices will have the size 2x2.

Assembling the stiffness and mass matrices: To assemble the global stiffness matrix of the MRF system, the direct stiffness method will be used. In this approach, the contributions of different beam-column elements are summed up to yield stiffness coefficients for the global matrix. The stiffness coefficients, k_{ij} , for the beam-column element are shown in Figure 2. As a reminder, the meaning of the stiffness coefficient k_{ij} is the "force" in the direction of DOF 'i' given a unit "displacement" in the direction of DOF 'j'. The "force" in this case refers to either a force or a moment, while the "displacement" is either a translation or rotation.

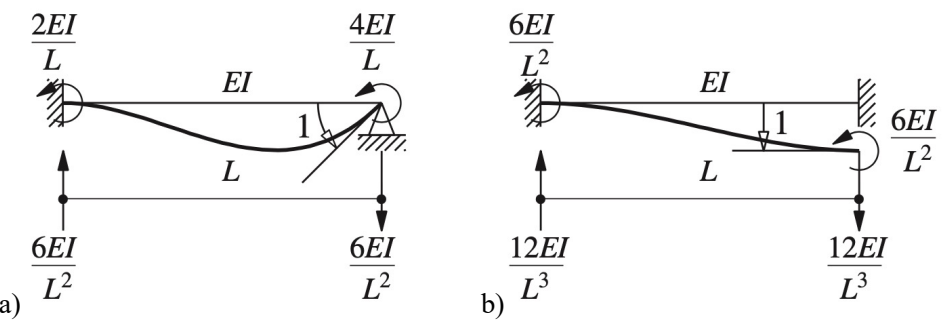


Figure 2. Stiffness coefficients, k_{ij} , for a linearly elastic beam-column element: a) coefficients for joint rotation; b) coefficients for joint translation. Figure adapted from [1].

The above definition of the stiffness coefficient can be leveraged to directly assemble the stiffness matrix for the system. In particular, to obtain the global stiffness matrix coefficient K_{ij} we apply a unit "displacement" in the direction of the global degree-of-freedom 'i' while keeping all other DOFs fixed, i.e., with zero displacement. Figure 3 demonstrates this approach for DOFs 2 and 5, the remaining coefficients can be obtained in an analogous manner.

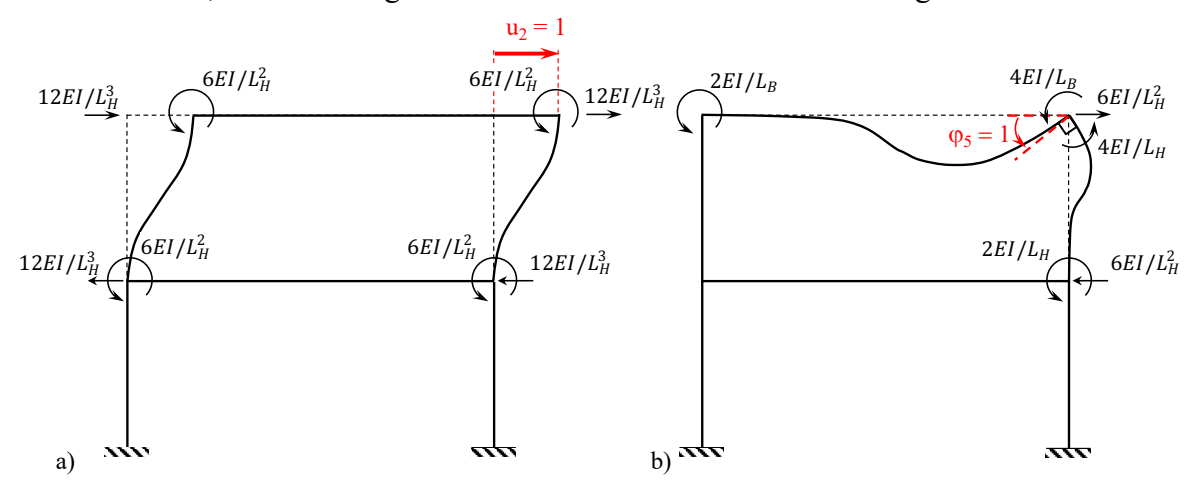


Figure 3. Stiffness coefficients, K_{ij} , for the MRF system: a) beam-column element contributions for coefficients K_{i2} ; b) beam-column element contributions for coefficients K_{i5} .

The 6x6 global stiffness matrix obtained using the direct stiffness approach for the 2story MRF is given in Figure 4. The stiffness coefficients from stiffness contributions shown in Figures 3a and 3b correspond to the second and fifth column in the global stiffness matrix, respectively. The factor of two that is multiplying the global matrix accounts for the fact that there are two identical MRF systems acting in parallel.

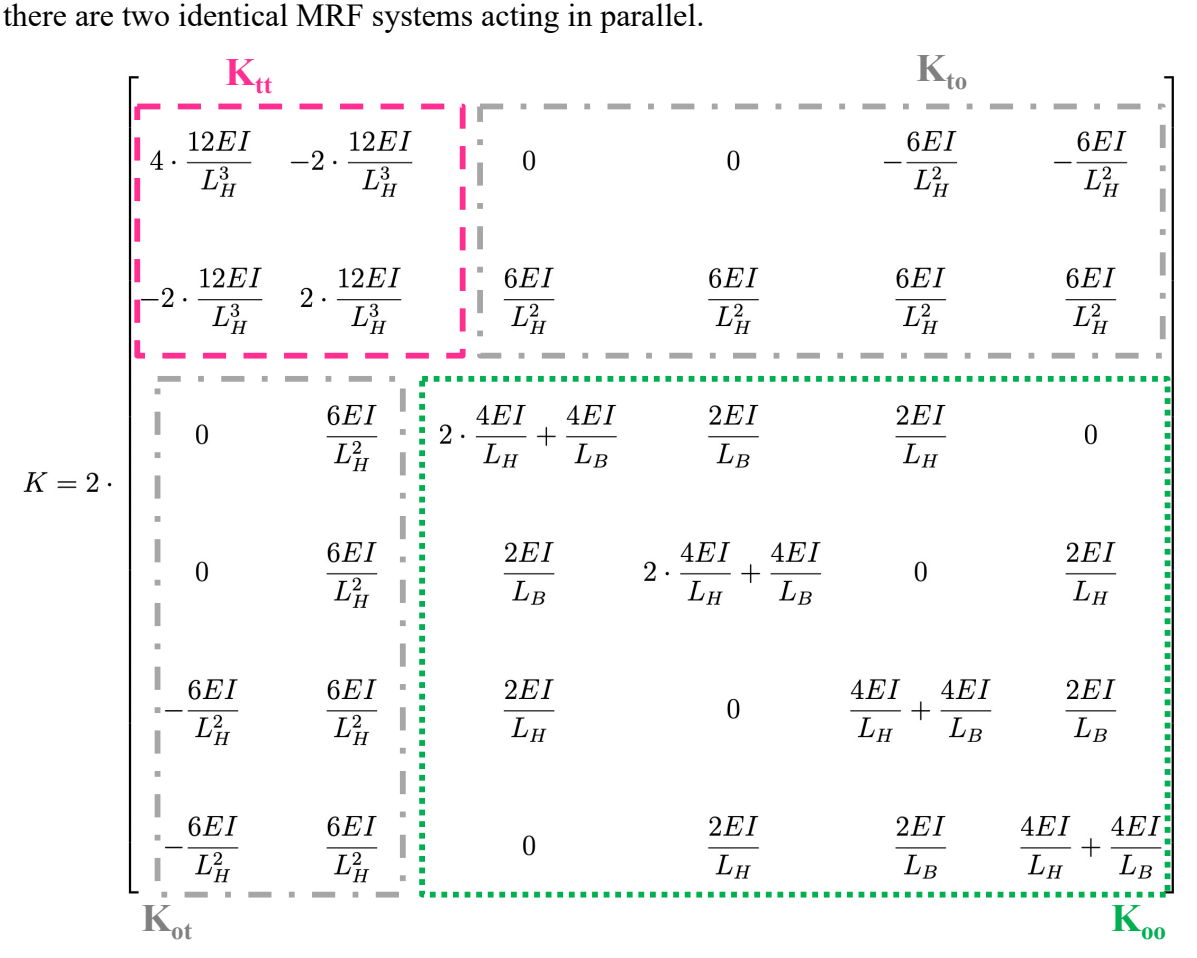


Figure 4. The global stiffness matrix of the 2-story MRF system.

Identified in Figure 4 are also the submatrices K_{tt} , K_{to} , and K_{oo} that can be used to perform static condensation using the following equation (e.g., chapter 9 in [1]):

$$\widehat{K} = K_{tt} - K_{ot}^T K_{oo}^{-1} K_{ot},$$

which yields the condensed stiffness matrix of the entire 2-story structure (units used are Newton for the force and meter for length):

$$\hat{\mathbf{K}} = \begin{bmatrix} 172.969 & -69.726 \\ -69.726 & 46.173 \end{bmatrix}.$$

Given that a lumped mass approximation is used herein, assembling the mass matrices is straightforward. Specifically, the matrices are diagonal with masses assigned to dynamic DOFs only, as shown in Figure 5. The masses m_1 and m_2 represent the masses lumped to the first and second floors respectively:

$$m_1 = 4m_{ball} + 2m_{spring, short} + 2m_{spring, long} + m_{slab} + 8m_{stiffener} = 0.142kg,$$

 $m_2 = 4m_{ball} + 2m_{spring, short} + 2m_{spring, long} + m_{slab} + 4m_{stiffener} = 0.133kg.$

Figure 5. The global mass matrix of the 2-story MRF system: a) the full mass matrix; b) condensed mass matrix for the dynamic DOFs.

Computing natural periods and mode shapes: Once the system-level stiffness and mass matrices have been assembled, eigenvalue analysis can be performed to determine the natural periods and mode shapes for the 2-story structure. In particular, the following equation represents the eigenvalue problem (chapter 10 in [1]):

$$\boldsymbol{k}\phi_n = \boldsymbol{m}\phi_n\omega_n^2 \,, \quad (1)$$

where ω_n^2 is the nth eigenvalue, while ϕ_n is the nth eigenvector. To solve the eigenvalue problem using, e.g., python or Matlab packages, the equation (1) needs to be converted to the standard eigenvalue problem of the form:

$$Av = \lambda v$$
, (2)

where A is the matrix for which the eigenvalues and eigenvectors are being computed, v is the eigenvector, and λ is the eigenvalue. The reformatting can be achieved by pre-multiplying the equation (1) by the inverse of the mass matrix. This process yields the following natural periods and mode shapes (mode shapes scaled to unit value at DOF 2 are visualized in Figure 6):

 $T_1 = 0.588$ s, $T_2 = 0.165$ s, (4)

Figure 6. Visualization of the mode shapes for the 2-story MDOF system.

PART 2 - Damping:

<u>Estimation of the damping ratio</u>: The results of experimental measurements of the free vibration can be used to estimate the damping characteristics of the building. Shown in Figure 7 is the measured response of the free vibration for the horizontal displacements of the first and second floors (i.e., displacements for DOFs u_1 and u_2). Indicated with red triangles and x-shaped markers are the peaks of the response. These peaks can be used to estimate the damping from the logarithmic decrement (chapter 2 in [1]):

$$\delta = (1/j) \ln (u^i/u^{i+j}) = 2\pi \zeta,$$
 (6)

where u^i and u^{i+j} represent the i^{th} and $i+j^{th}$ peak of the response, δ is the logarithmic decrement, j is the number of cycles over which the motion decreases, and ζ is the damping ratio being estimated. By applying the equation (6) to the measured displacements of the first and the second floors and taking the mean value, the damping ratio $\zeta \approx 0.07$ is obtained.

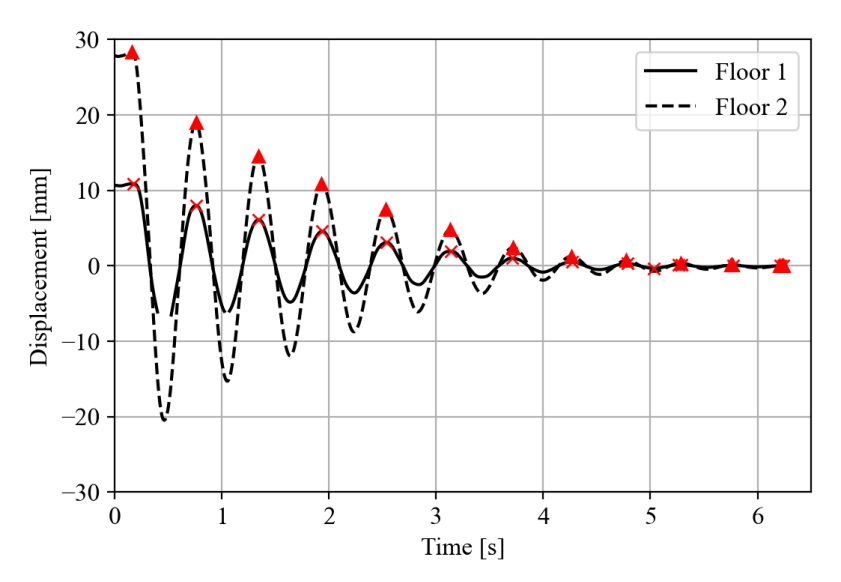


Figure 7. Damping estimation from the measured free vibration response.

Assemble the Rayleigh damping matrix: The damping matrix used herein will be the stiffness and mass proportional damping matrix, i.e., the Rayleigh damping matrix. The key related modelling consideration is to assign the desired damping ratio ζ at two circular frequencies ω_1 and ω_2 from which the mass matrix factor, a_0 , and stiffness matrix factor, a_1 , can be computed as follows:

$$a_0 = \zeta \left(\frac{2\omega_1\omega_2}{\omega_1 + \omega_2}\right), a_1 = \frac{2\zeta}{\omega_1 + \omega_2}.$$
 (7)

Once the factors a_0 and a_1 are computed, the damping matrix for the system can be obtained as:

$$\mathbf{C} = a_0 \widehat{\mathbf{M}} + a_1 \widehat{\mathbf{K}}$$

Given that the 2-story model is responding in the first mode for the free vibration (see video '2dof_mrf_free_vib_video.avi'), the estimated damping ratio corresponds to the damping in the first mode. Herein we will assume that the damping ratio in the second mode takes the same value. In other words, when computing the coefficients a_0 and a_1 we will use circular frequencies based on natural periods T_1 and T_2 of the two-story frame. This yields

values of $a_0 = 1.205067$ and $a_1 = 0.002961$. However, note that the selection of circular frequencies ω_1 and ω_2 is a modelling choice and hence need not be based on natural periods of the structure.

Checking the eigenvalue analysis results: The free vibration response measurement offers an opportunity to check some of the modal analysis values computed in Part I. As mentioned previously, given that the structure is vibrating in the first mode the fundamental period can be estimated from the zero-crossings, as shown in Figure 8. The estimate of the fundamental period $T^* = 0.578$ s was obtained as the average value between the zero-crossings indicated with red star-shaped markers in the figure. This value is within 2% difference of the fundamental period $T_1 = 0.588$ s computed using the eigenvalue analysis.

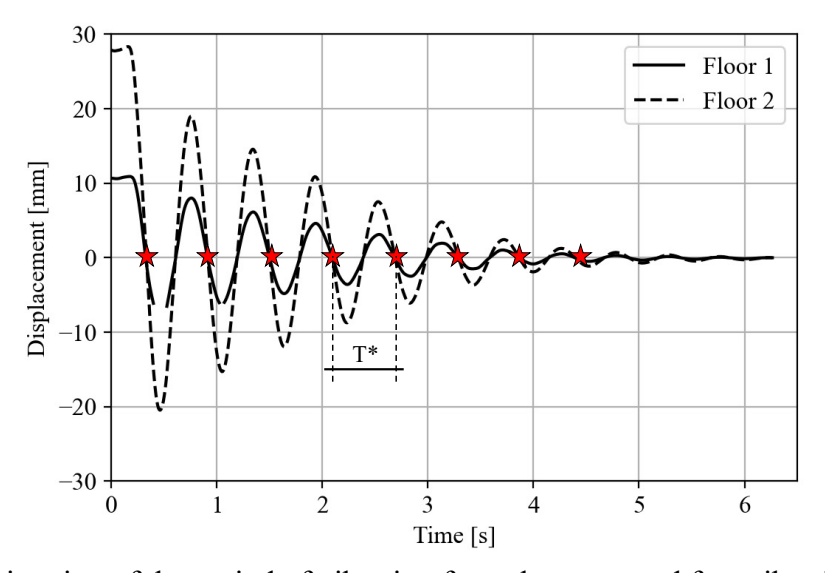


Figure 8. Estimation of the period of vibration from the measured free vibration response.

Given the value of the period T^* it is possible to compute the corresponding modal stiffness K_1 * using the modal mass M_1 as follows:

$$M_{1} = \phi_{1}^{T} \widehat{\mathbf{M}} \phi_{1} = \begin{cases} 0.40632 \\ 0.91373 \end{cases}^{T} \widehat{\mathbf{M}} \begin{cases} 0.40632 \\ 0.91373 \end{cases} = 0.13455, (8)$$

$$K_{1}^{*} = \left(\frac{2\pi}{T^{*}}\right)^{2} M_{1} = 15.8826. (9)$$

The modal stiffness K_1 can also be computed in the analogous way using the condensed stiffness matrix $\hat{\mathbf{K}}$ which yields $K_1 = 15.3325$. Note that in this computation the same eigenvectors are used as when computing K_I^* , but the computation is based on the condensed stiffness matrix rather than on the modal mass. The difference between K_I and K_I^* is around 3.5% which is an independent check giving some support that the stiffness matrix and eigenvalue analyses computed in Part I are correct.

PART 3 – Response to seismic excitation:

Response spectrum of the El Centro ground motion: The pseudo-acceleration, $S_a(T)$, response spectrum for the El Centro earthquake ground motion is shown in Figure 9. The graph is plotted in the log-log scale where the two structural periods of 0.588s and 0.165s are indicated with vertical lines. The corresponding values of the spectral accelerations are also shown on the

figure with red star-shaped markers. Note that the pseudo-acceleration is about 50% smaller at the fundamental mode compared to the second modal period.

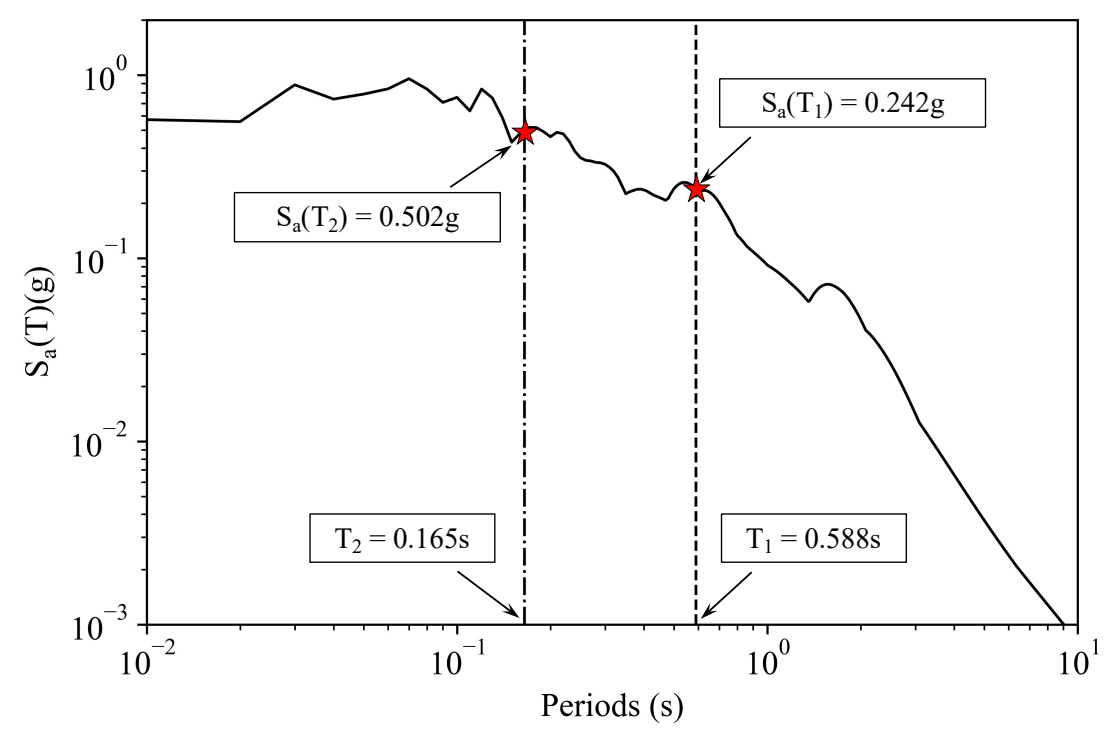


Figure 9. Pseudo-acceleration, $S_a(T)$, response spectrum for the El Centro earthquake ground motion.

<u>Response history analysis (RHA) using modal superposition</u>: The fundamental assumption of the modal superposition is that the structure is responding in a linear elastic manner. If this is the case, then the equations of motion of an MDOF with classical damping can be uncoupled and solved independently for a series of SDOF systems. The total response is obtained by combining the SDOF responses using the modal participation factors:

$$\boldsymbol{u}(t) = \sum_{n=1}^{2} \phi_n \Gamma_n \, \mathbf{D}_n(t), \quad (10)$$

where ϕ_n are the mode shape vectors, Γ_n are the modal participation factors, and $D_n(t)$ represents the response history of an SDOF with the period T_n and damping ratio ζ_n to the input ground motion.

Note that in the equation (10), the only quantity that is a function of time is $D_n(t)$, i.e., the time response of the SDOF system which can be obtained using a numerical integration scheme such as the Newmark's method. The ϕ_n is a vector of constants (obtained in Part I), while the modal participation factors Γ_n can be obtained using the following equations:

$$\Gamma_n = L_n/M_n, \ L_n = \phi_n^T \widehat{\boldsymbol{M}} \ \iota, \ M_n = \phi_n^T \widehat{\boldsymbol{M}} \phi_n, (11)$$

where the $t = [1 \ 1]^T$ is the influence vector for the translational ground motion. Using the equation (11), the following modal participation factors are obtained for the 2-story MRF system: $\Gamma_1 = 1.3324$, $\Gamma_2 = 0.5076$. The comparison between displacements obtained using RHA and the measurements is shown in Figure 10. While there are some minor differences, the computed responses closely follow the measurements.

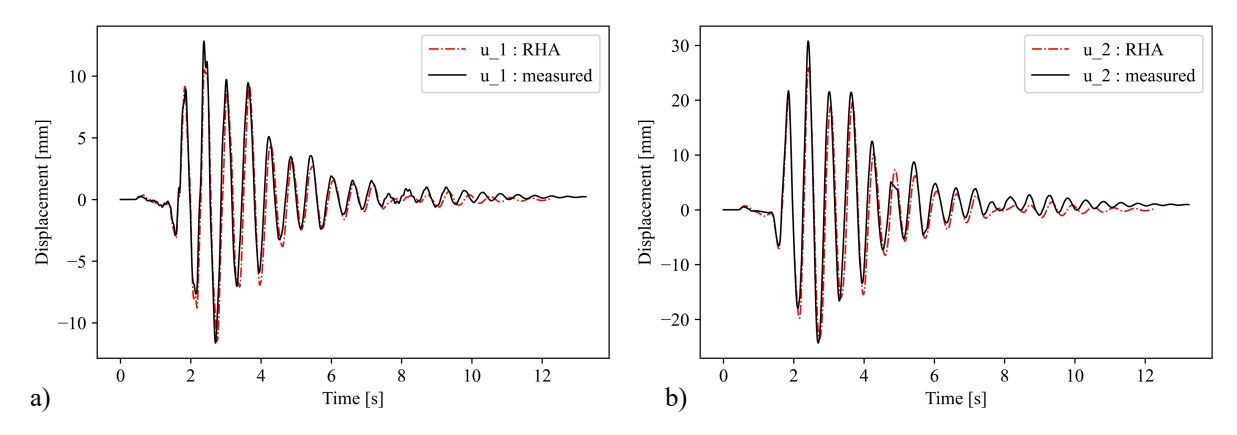


Figure 10. Comparison of the measured and computed displacements: a) first story; b) second story.

<u>A note on using the recorded earthquake ground motion as an input for the small-scale shake table</u>: The El Centro ground motion used in this project is shown in Figure 11. Specifically, the figure shows the ground motion as recorded during the earthquake with the ground accelerations and ground displacements shown in Figure 11a and 11b, respectively. It can be seen that the PGA (peak ground acceleration) equals about 0.5g while the maximum ground displacement is on the order of 50cm.

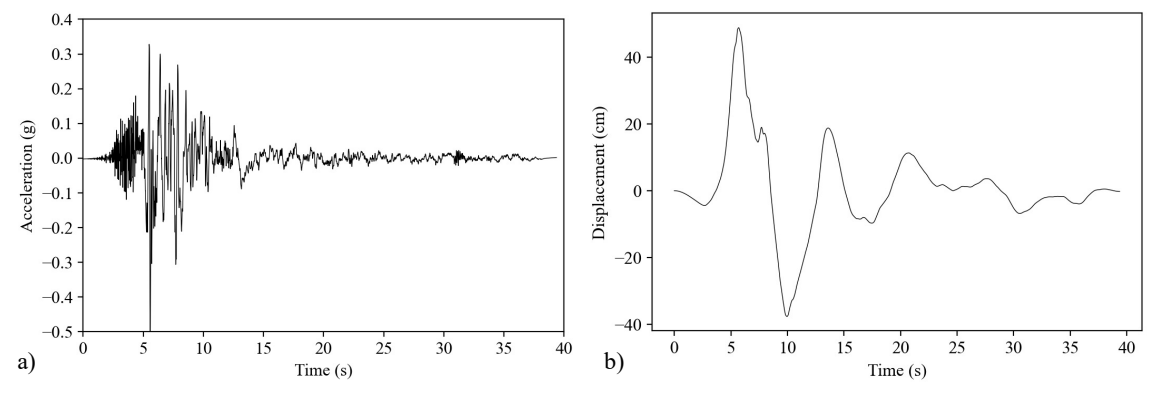


Figure 11. El Centro ground motion record: a) ground acceleration; b) ground displacement.

Since the stroke of the shake table is +/- 7.5cm, this small-scale table cannot directly reproduce the ground motion as it was recorded. Hence, the record needs to be scaled in a way that preserves the accelerations but so that the displacements do not exceed the capabilities of the shake table. Shown in Figure 12 is the shake table response that corresponds to the El Centro ground motion after scaling.

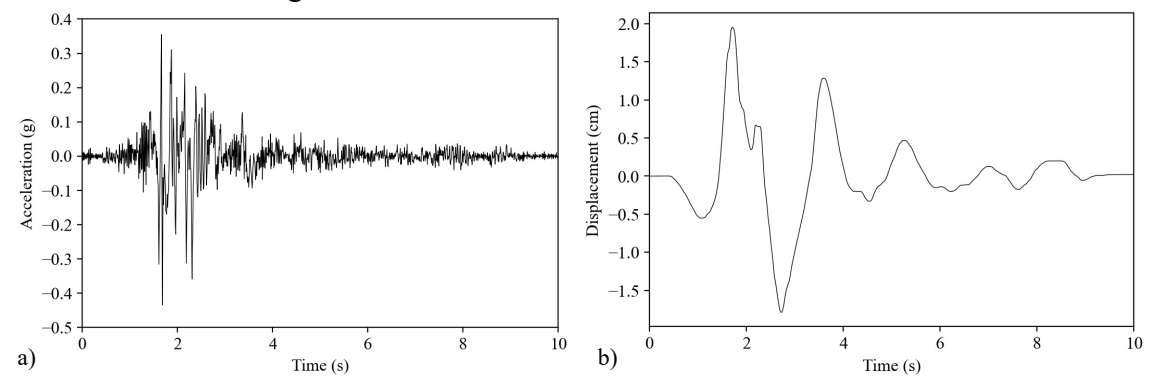


Figure 12. Shake table response to the input motion: a) acceleration; b) displacement.

Note that the shapes of acceleration and displacement time series in Figure 12 look similar to the corresponding data in Figure 11. Furthermore, the amplitudes of the two acceleration time series are similar. In contrast, the displacements after scaling are much smaller compared to the recorded motion. In particular, the maximum displacement of the shake table response is around 2cm – which can be accommodated by the stroke of the table – as compared to the 50cm of the recorded motion. Also note that, as the result of this scaling process, the length of the time series changed from about 40s to around 10s. This is necessary so as to keep the accelerations between the motions in close agreement while reducing the displacements. Some additional information about this scaling process is available from the shake table manufacturer: https://www.quanser.com/blog/scaling-earthquakes-quanser-way/.

Finally, some minor differences in the acceleration time series between Figures 11 and 12 are due to the fact that Figure 12 shows the measured response of the shake table and not the scaled ground motion which was provided as an input to the controller that shakes the table. In other words, the motion of the shake table is not exactly the same as the signal provided as the input. At the same time, we are interested in the ground motion that is shaking the model and are hence using the measured acceleration of the shake table as the basis of the analyses in this project.

References:

[1] Chopra, A.K. "Dynamics of structures: theory and applications to earthquake engineering", 4th Edition, Prentice Hall, 2012